Tspan18 is a novel regulator of the Ca2+ channel Orai1 and von Willebrand factor release in endothelial cells

Noy, Peter J.; Gavin, Rebecca L.; Colombo, Dario; Haining, Elizabeth J.; Reyat, Jasmeet S.; Payne, Holly; Thielmann, Ina; Lokman, Adam B.; Neag, Georgiana; Yang, Jing; Lloyd, Tammy; Harrison, Neale; Heath, Victoria L.; Gardiner, Chris; Whitworth, Katharine M.; Robinson, Joseph; Koo, Chek Z.; Di Maio, Alessandro; Harrison, Paul; Lee, Steven P.

DOI:
10.3324/haematol.2018.194241

Ferrata Storti Foundation

Tspan18 is a novel regulator of the Ca^{2+} channel Orai1 and von Willebrand factor release in endothelial cells

Peter J. Noy,[1] Rebecca L. Gavin,[1] Dario Colombo,[2] Elizabeth J. Haining,[2] Jasmeet S. Reyat,[1] Holly Payne,[2] Ina Thielmann,[3] Adam B. Lokman,[2] Georgiana Neag,[2] Jing Yang,[1] Tammy Lloyd,[1] Neale Harrison,[1] Victoria L. Heath,[2] Chris Gardiner,[4] Katharine M. Whitworth,[5] Joseph Robinson,[5] Chek Z. Koo,[1] Alessandro Di Maio,[1] Paul Harrison,[6,7] Steven P. Lee,[5] Francesco Michelangeli,[8] Neena Kalia,[2,9] G. Ed Rainger,[2] Bernhard Nieswandt,[3] Alexander Brill,[2,9,10] Steve P. Watson[2,9] and Michael G. Tomlinson[1,9]

[1]School of Biosciences, College of Life and Environmental Sciences, University of Birmingham, Birmingham, UK; [2]Institute of Cardiovascular Sciences, College of Medical and Dental Sciences, University of Birmingham, Birmingham, UK; [3]University Hospital Würzburg and Rudolf Virchow Center for Experimental Biomedicine, Würzburg, Germany; [4]Department of Haematology, University College London, London, UK; [5]Institute of Immunology and Immunotherapy, Cancer Immunology and Immunotherapy Centre, University of Birmingham, Birmingham, UK; [6]Scar Free Foundation for Burns Research, Queen Elizabeth Hospital Birmingham, University Hospitals Birmingham National Health Service (NHS) Foundation Trust, Birmingham, UK; [7]Institute of Inflammation and Ageing, University of Birmingham, Birmingham, UK; [8]Department of Biological Sciences, University of Chester, Chester, UK; [9]Centre of Membrane Proteins and Receptors (COMPARE), Universities of Birmingham and Nottingham, Birmingham-Nottingham, UK and [10]Department of Pathophysiology, Sechenov First Moscow State Medical University, Moscow, Russia

Haematologica 2019
Volume 104(9):1892-1905

Correspondence:

MICHAEL G. TOMLINSON
m.g.tomlinson@bham.ac.uk

Received: March 26, 2018.

Accepted: December 19, 2018.

Pre-published: December 20, 2018.

doi:10.3324/haematol.2018.194241

Check the online version for the most updated information on this article, online supplements, and information on authorship & disclosures: www.haematologica.org/content/104/9/1892

ABSTRACT

Ca^{2+} entry *via* Orai1 store-operated Ca^{2+} channels in the plasma membrane is critical to cell function, and Orai1 loss causes severe immunodeficiency and developmental defects. The tetraspanins are a superfamily of transmembrane proteins that interact with specific 'partner proteins' and regulate their trafficking and clustering. The aim of this study was to functionally characterize tetraspanin Tspan18. We show that Tspan18 is expressed by endothelial cells at several-fold higher levels than most other cell types analyzed. Tspan18-knockdown primary human umbilical vein endothelial cells have 55-70% decreased Ca^{2+} mobilization upon stimulation with the inflammatory mediators thrombin or histamine, similar to Orai1-knockdown. Tspan18 interacts with Orai1, and Orai1 cell surface localization is reduced by 70% in Tspan18-knockdown endothelial cells. Tspan18 overexpression in lymphocyte model cell lines induces 20-fold activation of Ca^{2+}-responsive nuclear factor of activated T cell (NFAT) signaling, in an Orai1-dependent manner. Tspan18-knockout mice are viable. They lose on average 6-fold more blood in a tail-bleed assay. This is due to Tspan18 deficiency in non-hematopoietic cells, as assessed using chimeric mice. Tspan18-knockout mice have 60% reduced thrombus size in a deep vein thrombosis model, and 50% reduced platelet deposition in the microcirculation following myocardial ischemia-reperfusion injury. Histamine- or thrombin-induced von Willebrand factor release from endothelial cells is reduced by 90% following Tspan18-knockdown, and histamine-induced increase of plasma von Willebrand factor is reduced by 45% in Tspan18-knockout mice. These findings identify Tspan18 as a novel regulator of endothelial cell Orai1/Ca^{2+} signaling and von Willebrand factor release in response to inflammatory stimuli.

Introduction

The tetraspanins are a superfamily of proteins containing four transmembrane regions that interact with and regulate the trafficking, lateral mobility and clustering of specific 'partner proteins'. These include signaling receptors, adhesion molecules and metalloproteinases.[1-3] Recently, the first crystal structure of a tetraspanin, CD81, demonstrated a cone-shaped structure with a cholesterol-binding cavity within the transmembranes.[4] Molecular dynamics simulations suggest that cholesterol removal causes a dramatic conformational change, whereby the main extracellular region swings upwards.[4] This raises the possibility that tetraspanins function as 'molecular switches' to regulate partner protein function *via* conformational change, and suggests that tetraspanins are viable future drug targets.

Tetraspanin Tspan18 was previously studied in chick embryos, in which it stabilizes expression of the homophilic adhesion molecule cadherin 6B to maintain adherens junctions between premigratory epithelial cranial neural crest cells.[5,6] Transcriptional Tspan18 downregulation is required for loss of cadherin 6B expression, breakdown of epithelial junctions, and neural crest cell migration. However, Tspan18 knockdown has no major effect on chick embryonic development.[5,6] The function of Tspan18 in humans or mice has still not been studied.

Store-operated Ca^{2+} entry (SOCE) through the plasma membrane Ca^{2+} channel Orai1 is essential for the healthy function of most cell types.[7] Loss of SOCE results in severe immunodeficiency that requires a bone marrow transplant for survival. Further symptoms include ectodermal dysplasia and impaired development of skeletal muscle.[7] The process of SOCE is biphasic. The first step is initiated following the generation of the second messenger inositol trisphosphate (IP3) from upstream tyrosine kinase or G protein-coupled receptor signaling. IP3 induces the transient release of Ca^{2+} from endoplasmic reticulum (ER) stores *via* IP3 receptor channels.[8] Depletion of Ca^{2+} is detected by the ER-resident dimeric Ca^{2+}-sensor protein STIM1, which then undergoes a conformational change and interacts with Orai1 hexamers in the plasma membrane.[9,10] STIM1 binding induces Orai1 channel opening and clustering *via* a mechanism that is not fully understood, allowing Ca^{2+} entry across the plasma membrane.[9,10] The resulting increase in intracellular Ca^{2+} concentration is relatively large and sustained, sufficient to activate a variety of signaling proteins, including the widely-expressed nuclear factor of activated T-cell (NFAT) transcription factors.[8]

Endothelial cells line all blood and lymphatic vessels and play a central role in hemostasis and in thrombo-inflammation, in which inflammatory cells contribute to thrombosis.[11,12] In the thrombo-inflammatory disease deep vein thrombosis, blood flow stagnation induced by prolonged immobility, for example, is the trigger for endothelial cells to exocytose Weibel-Palade storage bodies *via* a mechanism involving Ca^{2+} signaling.[13,14] This releases the multimeric glycoprotein von Willebrand factor (vWF) and the adhesion molecule P-selectin, which recruit platelets and leukocytes, respectively. vWF-bound platelets provide a pro-coagulant surface for activation of clotting factors and thrombin generation, neutrophils release neutrophil extracellular traps, and mast cells release endothelial-activating substances.[15-17] This series of thrombo-inflammatory events leads to formation of a blood clot which occludes the vein, and can cause death by pulmonary thromboembolism.

The aim of this study was to determine the function of tetraspanin Tspan18 in humans and mice. We found that Tspan18 is highly expressed by endothelial cells, interacts with Orai1, and is required for its cell surface expression and SOCE function. As a consequence, Tspan18-deficient endothelial cells have impaired Ca^{2+} mobilization and release of vWF upon activation induced by inflammatory mediators, and Tspan18-knockout mice are protected from deep vein thrombosis and myocardial ischemia-reperfusion injury, and have defective hemostasis.

Methods

Ethics statement

Procedures in Birmingham were approved by the UK Home Office according to the Animals (Scientific Procedures) Act 1986, and those in Würzburg by the district government of Lower Frankonia (Bezirksregierung Unterfranken).

Mice

Tspan18$^{-/-}$ mice were generated by Genentech/Lexicon Pharmaceuticals on a mixed genetic background of 129/SvEvBrd and C57BL/6J.[18] They were purchased from the Mutant Mouse Regional Resource Center and bred as heterozygotes to generate litter-matched Tspan18$^{-/-}$ and Tspan18$^{+/+}$ pairs. Radiation fetal liver chimeric mice were generated as described.[19]

Antibodies

Anti-epitope tag antibodies were mouse anti-Myc 9B11 and rabbit anti-Myc 71D10 (Cell Signaling Technology), mouse anti-FLAG M2 and rabbit anti-FLAG (Sigma). Other antibodies were mouse anti-human calnexin AF18 (Abcam), rat anti-mouse CD16/32 (BioLegend), CD41 (eBioscience) and panendothelial cell antigen MECA-32 (BD Pharmingen), mouse anti-ERK1/2 and rabbit anti-phospho-ERK1/2 (Cell Signaling Technology) and rabbit anti-human vWF (GE Healthcare). Biotinylated isolectin GS-IB4 glycoprotein was from ThermoFisher Scientific.

Expression constructs

The NFAT/AP1-luciferase transcriptional reporter construct has been described previously.[20,21] pEF6/Myc-His (mock) and pEF6/Myc-His/lacZ were from Invitrogen. N-terminal FLAG-tagged tetraspanin constructs were generated in pEF6/Myc-His as described.[22,23] pcDNA3.1 Myc-His-tagged human Orai1 and MO70-FLAG-tagged human Orai1 E106Q were from Addgene[24] and the dominant-active calcineurin was as described.[25]

Cell culture and transfections

Detailed information on cell cultures is provided in the *Online Supplementary Appendix*. Wild-type and IP3 receptor-deficient DT40 chicken B-cell lines,[26] and Jurkat human T-cell line, were transfected by electroporation.[21] Human embryonic kidney (HEK)-293T (HEK-293 cells expressing the large T-antigen of simian virus 40) and the human HeLa epithelial cell line were transfected using polyethylenimine (Sigma)[27] and Lipofectamine 2000 (Invitrogen),[28] respectively. Human umbilical vein endothelial cells (HUVEC)[29] were transfected with 10 nM

Silencer Select siRNA duplexes (Invitrogen) using Lipofectamine RNAiMAX (Invitrogen).

Quantitative real-time polymerase chain reaction

Quantitative real-time polymerase chain reaction (qPCR) was performed using TaqMan assays for Tspan18, Orai1, Orai2, Orai3, 18S and GAPDH.[30] Details are available in the *Online Supplementary Appendix*.

Lentiviral transduction

Human umbilical vein endothelial cells were lentivirally transduced with Orai1-Myc as described.[31] Details are available in the *Online Supplementary Appendix*.

Nuclear factor of activated T-cell/AP-1-luciferase transcriptional reporter assay

The NFAT/AP-1-luciferase assay, and β-galactosidase assay to normalize for transfection efficiency, were as described.[21]

Co-immunoprecipitation

A detailed description of co-immunoprecipitation from transfected HEK-293T cell lysates[22] is provided in the *Online Supplementary Appendix.*

Immunofluorescence microscopy

Detailed information is provided in the *Online Supplementary Appendix*. In brief, cells were prepared as described[29] and the Manders' coefficients (M1 and M2) were used as the co-localization measure.[32] Ear vasculature was imaged and quantified as described.[33,34]

Immunohistochemistry

Immunohistochemistry was as described;[35] details are available in the *Online Supplementary Appendix*.

Intracellular Ca^{2+}

Human umbilical vein endothelial cells were loaded with Fluo-4 NW dye according to the manufacturer's instructions (Molecular Probes). Fluorescence was measured every 3 seconds for 5 minutes using a FlexStation fluorescence reader (Molecular Devices), and thrombin (1 U/mL), histamine (20 μM) or ionomycin (10 μM) were injected after acquiring a baseline for 30 seconds.

ELISA and coagulation time assays

Detailed information is provided in the *Online Supplementary Appendix.*

Platelet aggregation and adhesion to human umbilical vein endothelial cells

Platelet assays were as described;[36,37] detailed information is provided in the *Online Supplementary Appendix.*

In vivo assays

Mouse models were as described;[13,37-39] detailed information is in the *Online Supplementary Appendix*.

Results

Tspan18 is expressed by endothelial cells

A lack of effective antibodies to many tetraspanins is a current problem in the tetraspanin field. This may be due to their relatively small size, high degree of sequence conservation during evolution, and compact 4-transmembrane structure.[4] For example, no Tspan18 antibodies have been published, and commercially-available antibodies are made to Tspan18 peptides and do not detect full-length Tspan18 when rigorously tested (*MG Tomlinson, 2019, unpublished manuscript*). Therefore, to characterize the Tspan18 expression profile, mouse tissues were tested by qPCR. Tspan18 mRNA was most highly expressed in lung and at lower levels in other tissues (Figure 1A). Analyses of published transcriptomic data[40] showed that Tspan18 was most highly expressed by endothelial cells compared to other mouse lung cell types (Figure 1B). Similar analyses of transcriptomic data from mouse brain[41] also showed relatively strong endothelial expression of Tspan18 (Figure 1C). Consistent with this, qPCR showed that Tspan18 was expressed by primary HUVEC and the human microvascular endothelial HMEC-1 cell line (Figure 1D). Tspan18 expression was low or absent on most other cell types tested, although peripheral blood leukocytes expressed comparable levels to HUVEC (Figure 1D). In transcriptomic data from the Human Protein Atlas (*www.proteinatlas.org*), Tspan18 was expressed by most human tissues at a level between 10 and 70 tags per million, but in cell lines was only expressed at 10 or greater tags per million by HUVEC and 8 of the other 64 cell types analyzed.[42]

Tspan18 is required for Ca^{2+} signaling in primary human endothelial cells

To investigate Tspan18 function, its expression in HUVEC, which is a widely-used primary human endothelial cell model, was knocked-down using two different siRNA duplexes. Subsequent analyses revealed a 60% reduction in peak Ca^{2+} elevation in response to the inflammatory mediator thrombin (Figure 2A). A similar defect was observed in response to histamine (Figure 2B). Positive control ionomycin treatment gave a sustained intracellular Ca^{2+} response in all samples (Figure 2C) and effective knockdown was confirmed by qPCR (Figure 2D). Functionality of thrombin and histamine receptors was confirmed by anti-phospho-ERK1/2 mitogen-activated protein kinase (MAPK) western blotting, as this was not affected by Tspan18 knockdown (Figure 2E).

Tspan18 promotes Ca^{2+}-responsive nuclear factor of activated T-cell signaling in lymphocyte cell lines

To investigate the mechanism by which Tspan18 regulates Ca^{2+} signaling, a more tractable cell line system was established, namely DT40 cells that are derived from chicken B cells. In this cell line, a transfected NFAT/adapter protein 1 (AP-1) transcriptional luciferase reporter can be used as a readout for Ca^{2+} signaling downstream of transfected membrane proteins.[21,43] Transfection of a FLAG epitope-tagged Tspan18 expression construct was sufficient to induce robust NFAT/AP-1 activation (Figure 3A). As controls, five other FLAG-tagged tetraspanins (CD9, CD63, CD151, Tspan32 and Tspan9) were chosen because they represent a diverse range of tetraspanins based on sequence identities.[22] These did not induce NFAT/AP-1 activation, despite their substantially higher expression than Tspan18 as assessed by anti-FLAG western blotting (Figure 3A).

Despite the fact that the NFAT/AP-1 promoter can be activated by Ca^{2+} signaling, it is maximally activated by combined Ca^{2+} signaling and MAPK; Ca^{2+} activates NFAT and MAPK activates AP-1. To determine whether

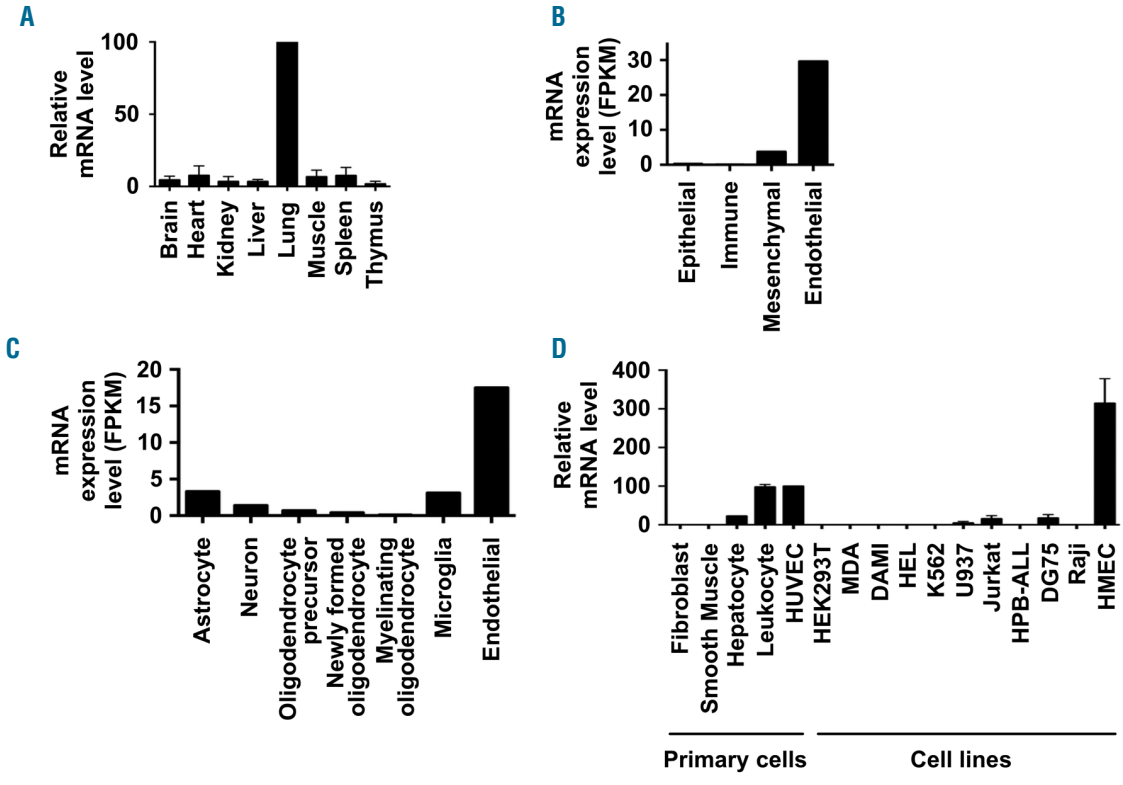

Figure 1. Tspan18 is highly expressed by endothelial cells. (A) Quantitative real-time polymerase chain reaction (qPCR) was carried out for Tspan18 using cDNA derived from a panel of mouse tissues. Data were normalized for the HPRT housekeeping gene and adjusted such that the lung value was 100 in each experiment. Error bars represent Standard Error of Mean from three independent tissue samples. (B) RNA-Seq data from major cell types in mouse lung, generated by Du *et al.*,[40] was used to show Tspan18 mRNA expression levels as fragments per kilobase of transcript sequence per million mapped fragments (FPKM). (C) RNA-Seq data from major cell types in mouse brain, generated by Zhang *et al.*,[41] was used to show Tspan18 mRNA expression levels as described in (B). (D) qPCR was carried out for Tspan18 on cDNA derived from a panel of primary human cells [dermal fibroblasts, aortic smooth muscle, hepatocytes, peripheral blood leukocytes from buffy coat and human umbilical vein endothelial cells (HUVEC)], and human cell lines (HEK-293T human embryonic kidney cells, MDA-MB-231 epithelial cells, DAMI megakaryocytic cells, HEL and K562 erythroleukemia cells, U937 monocytic cells, Jurkat and HPB-ALL T cells, DG75 and Raji B cells and HMEC-1 microvascular endothelial cells). Data were normalized for actin and adjusted such that the HUVEC value was 100 in each experiment. Error bars represent Standard Error of Mean from two independent cell samples.

Tspan18 activates Ca^{2+} signaling, MAPK or both, Tspan18-transfected DT40 cells were stimulated with the Ca^{2+} ionophore ionomycin or phorbol ester PMA to activate the MAPK pathway. PMA synergized with Tspan18 expression in activating NFAT/AP-1, but ionomycin did not (Figure 3B). As a positive control, combined PMA and ionomycin induced relatively strong NFAT/AP-1 activation in the presence or absence of Tspan18 (Figure 3B). The capacity of Tspan18 overexpression to induce NFAT/AP-1 activation was not restricted to DT40 B cells, since similar data were obtained in the human Jurkat T-cell line (Figure 3C). Taken together, these data suggest that Tspan18 promotes Ca^{2+} signaling and NFAT activation *via* a mechanism that is common to endothelial cells, B cells and T cells.

Tspan18-induced nuclear factor of activated T-cell activation requires functional Orai1 store-operated Ca^{2+} entry channels

To understand the mechanism by which Tspan18 promotes Ca^{2+} signaling, a series of NFAT/AP-1 reporter experiments were conducted in gene-knockout DT40 cells and using inhibitors and a dominant-interfering construct. Firstly, Tspan18-induced NFAT/AP-1 activation was found to be independent of the three IP3 receptors (Figure 3D). IP3 receptors release Ca^{2+} from ER stores in response to tyrosine kinase and G protein-coupled receptor activation, suggesting that Tspan18 does not operate on these pathways or IP3 receptors themselves. However, Tspan18 did not activate NFAT/AP-1 following chelation of extracellular Ca^{2+} (Figure 3E), or following treatment with the immunosuppressive drug cyclosporin A (Figure 3F), which prevents NFAT translocation to the nucleus by inhibiting its activatory phosphatase calcineurin. These data suggest that Tspan18 might induce Ca^{2+} entry *via* the SOCE channel Orai1, a major entry route for extracellular Ca^{2+} in non-excitable cells.[8] Consistent with this possibility, a dominant interfering form of Orai1 (E106Q), which multimerizes with endogenous Orai1 to yield a non-functional channel,[44-46] inhibited Tspan18-induced NFAT/AP-1 activation (Figure 3G). As a positive control to confirm that downstream NFAT signaling was still intact in the presence of dominant interfering Orai1, its inhibitory effect was overcome by the expression of an active form of calcineurin (Figure 3G). Therefore, Tspan18 may activate Ca^{2+} entry through the Orai1 SOCE pathway.

Tspan18 interacts with Orai1

To investigate whether Tspan18 interacts with Orai1, transfected epitope-tagged proteins were used because of

the lack of effective antibodies to Tspan18. To test for an interaction using co-immunoprecipitation, transfected HEK-293T cells were lyzed in 1% digitonin, a stringent detergent that has been used previously to identify tetraspanin-partner protein interactions.[22,47] FLAG-tagged Tspan18 co-immunoprecipitated with Myc-tagged Orai1, but five other control tetraspanins did not (Figure 4A). Moreover, Tspan18 and Orai1 co-localized when expressed in HeLa cells, at a level of approximately 90% pixel co-localization when assessed using the Manders' coefficient (Figure 4B). These data suggest that Tspan18 interacts with Orai1.

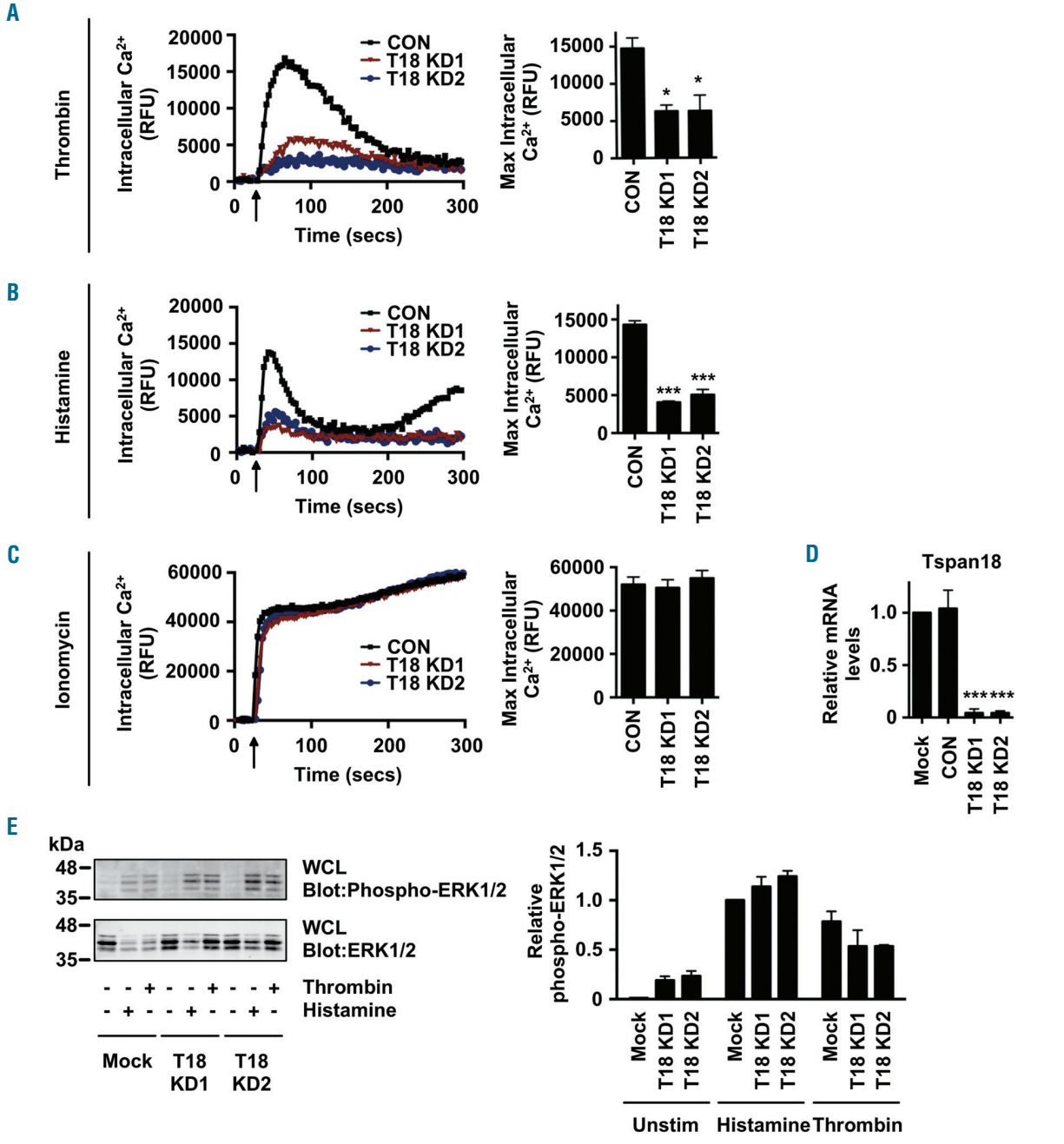

Figure 2. Tspan18-knockdown endothelial cells have impaired Ca^{2+} mobilization. (A-D) Human umbilical vein endothelial cells (HUVEC) were transfected with a negative control siRNA (CON) or with one of two independent siRNA targeting Tspan18 (T18 KD). After 48 hours, HUVEC were loaded with the Ca^{2+}-sensitive dye Fluo-4 NW and Ca^{2+} measurements taken using a FlexStation fluorescence reader during addition (arrow) of (A) 1 U/mL thrombin, (B) 20 μM histamine, or (C) 10 μM ionomycin. Representative Ca^{2+} traces are shown for Tspan18-knockdown HUVEC (left), with quantitation of maximum intracellular Ca^{2+} concentrations (right). Data were analyzed by one-way ANOVA with Dunnett's multiple comparisons test. Error bars represent the Standard Error of Mean (SEM) from three independent experiments. *P<0.05; ***P<0.001. (D) siRNA-transfected HUVEC from (A) to (C) were harvested, mRNA extracted, cDNA produced and Tspan18 mRNA levels were assessed by quantitative real-time polymerase chain reaction (qPCR). Data were normalized to 18S and actin as internal controls and adjusted such that the non-siRNA-transfected mock value was 1 in each experiment. Data were then normalized by logarithmic transformation, and analyzed by one-way ANOVA and Tukey's multiple comparison test. Error bars represent the Standard Error of the Mean from three independent experiments. ***P<0.001. (E) HUVEC were subjected to Tspan18 siRNA knockdown as described for (A-D), stimulated with 1 U/mL thrombin or 20 μM histamine for 5 minutes, then whole cell lysates were analyzed by western blotting with phospho-ERK1/2 and total ERK1/2 antibodies. (Left) Representative blots. (Right) Quantitation of three independent experiments. Error bars represent SEM. Knockdown efficiency was similar to that shown in (D) (*data not shown*). secs: seconds; RFU: relative fluorescence unit.

Orai1-knockdown endothelial cells have impaired Ca^{2+} mobilization and Orai1 surface expression requires Tspan18

To determine whether knockdown of Orai1 could phenocopy Tspan18 knockdown, intracellular Ca^{2+} mobilization was measured following siRNA-mediated knockdown of Orai1. This resulted in impaired Ca^{2+} mobilization in response to thrombin (Figure 5A) or histamine (Figure 5B). As a control, knockdown of the other Orai family members, Orai2 and Orai3, did not affect Ca^{2+} mobilization (Figure 5A and B), in agreement with previous studies on Orai proteins in HUVEC.[48,49] Positive control ionomycin treatment gave a sustained intracellular Ca^{2+} response in all samples (Figure 5C) and effective knockdown was confirmed by qPCR (Figure 5D-F).

A common mechanism of tetraspanin function is to regulate their partner proteins by facilitating their exit from the endoplasmic reticulum (ER) and trafficking to the cell surface.[1,50,51] To determine whether Orai1 localization could be regulated by Tspan18 in this manner, HUVEC were lentivirally transduced with Myc-Orai1 and transfected with control or Tspan18 siRNA duplexes, and Orai1 subcellular localization assessed by confocal microscopy. Orai1 was localized primarily to the cell periphery in control cells, but this was reduced following Tspan18 knockdown, with Orai1 partially co-localized with the ER marker calnexin (Figure 5G). Quantitative analyses showed that approximately 40% of Orai1 was

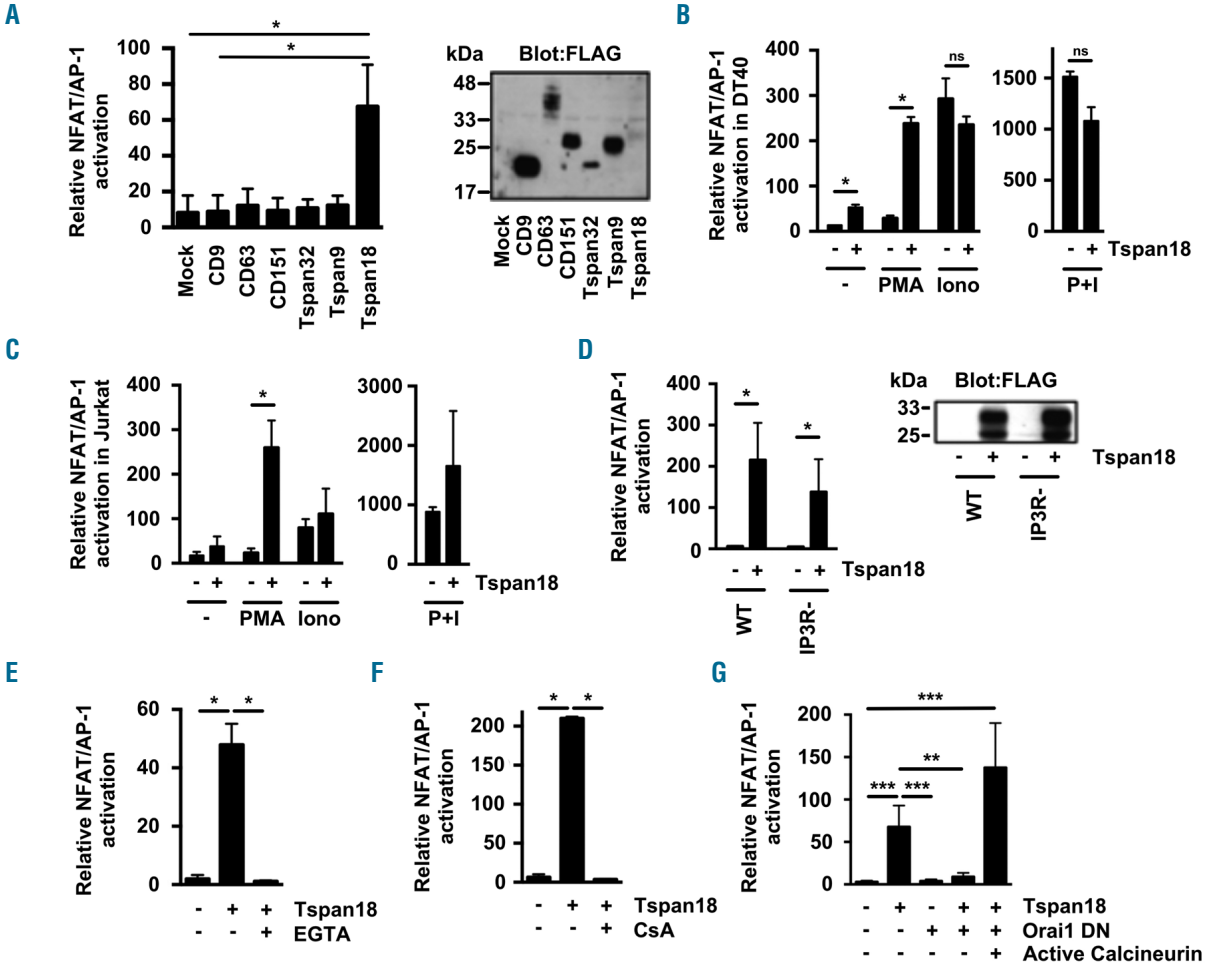

Figure 3. Tspan18 overexpression in cell lines activates Ca^{2+}-responsive NFAT signaling in an Orai1-dependant manner. (A) The DT40 B cell line was transfected with an NFAT/AP-1-luciferase reporter construct, a β-galactosidase expression construct driven by the elongation factor (EF)-1α promoter to control for transfection efficiency, and FLAG-tagged mouse tetraspanin constructs or empty vector control. At 24 hours (h) post transfection, cells were lyzed and assayed for luciferase and β-galactosidase. Luciferase data were normalized for β-galactosidase values (left). Whole cell lysates from these cells were separated by SDS-PAGE and blotted with an anti-FLAG antibody. (Right) Representative blot. (B and C) The DT40 B cell line (B) and the human Jurkat T cell line (C) were transfected with an NFAT/AP-1-luciferase reporter construct and β-galactosidase expression construct with (+) or without (-) FLAG-tagged mouse Tspan18. At 24 h post transfection cells were stimulated for 6 h with 50 ng/mL PMA or 1 μM ionomycin (Iono) (left), or both together (right). Luciferase assays were then performed as described in (A). (D) DT40 cells with (+) or without (-) expression of FLAG-tagged mouse Tspan18 were tested for NFAT/AP-1 luciferase activity as described in (A), but using cells with gene knockouts of the three IP3 receptors (IP3R-) in comparison to wild-type (WT) cells (left). Whole cell lysates were western blotted with an anti-FLAG antibody (right). (E and F) DT40 cells with (+) or without (-) expression of FLAG-tagged mouse Tspan18 were tested for NFAT/AP-1 luciferase activity as described in (A), except that cells were treated with 4 mM EGTA as a Ca^{2+} chelator (E) or with 2 μM cyclosporin A as a calcineurin inhibitor (F). (G) DT40 cells were transfected with FLAG-tagged human Tspan18 in the presence or absence of a dominant negative human Orai1 E106Q mutant construct, or a consitutively active human calcineurin construct. The experiment was conducted as described for (A). All luciferase data were corrected for β-galactosidase values, normalized by logarithmic transformation, and analyzed by one-way ANOVA and Tukey's multiple comparison test. *P<0.05; **P<0.01; ***P<0.001. Error bars represent the Standard Error of the Mean from at least three independent experiments. ns: not significant.

ER-localized in Tspan18 knockdown cells compared to 10-15% in control cells. This partial co-localization could be due to some Orai1 localization in the Golgi and/or trans-Golgi network, as shown by staining close to the nucleus, rather than the more extended perinuclear reticular staining of the ER (Figure 5G). These data support a role for Tspan18 in regulating Orai1 exit from the ER, and/or Golgi, and trafficking to the cell surface.

Tspan18 deficient mice have impaired hemostasis due to a defect in non-hematopoietic cells

To investigate Tspan18 function *in vivo*, Tspan18-knockout mice were acquired from Genentech/Lexicon Pharmaceuticals. These mice had been generated as part of a library of 472 knockouts,[18] but were functionally uncharacterized. Breeding of heterozygotes gave an equal proportion of male and female mice with Mendelian genotype ratios, and the mice bred successfully as homozygote knockouts (*data not shown*). Furthermore, Tspan18-knockout mice had normal body weights and whole blood cell counts (*data not shown*).

Tspan18-knockout mice were first evaluated for a hemostasis phenotype using a tail bleed assay. Most Tspan18-knockout mice bled more than wild-type littermates, demonstrating a significant disruption to hemostasis (Figure 6A). Some Tspan18-knockout mice did not bleed excessively (Figure 6A), indicating that the bleeding phenotype was variable. This variability could be due to genetic modifier *loci*, as demonstrated in mice deficient for the platelet collagen/fibrin receptor GPVI.[52] To determine whether impaired hemostasis was due to loss of Tspan18 from hematopoietic or non-hematopoietic cells, tail bleeding assays were performed on irradiated fetal liver chimeric mice. These demonstrated that the bleeding phenotype was due to Tspan18 loss from non-hematopoietic cells (Figure 6A), and suggests that a platelet defect is not responsible. Consistent with this, Tspan18-knockout platelets aggregated normally in response to collagen (Figure 6B) or thrombin (Figure 6C). Furthermore, prothrombin time and activated partial thromboplastin time tests showed that coagulation was similar for wild-type and Tspan18-knockout plasma

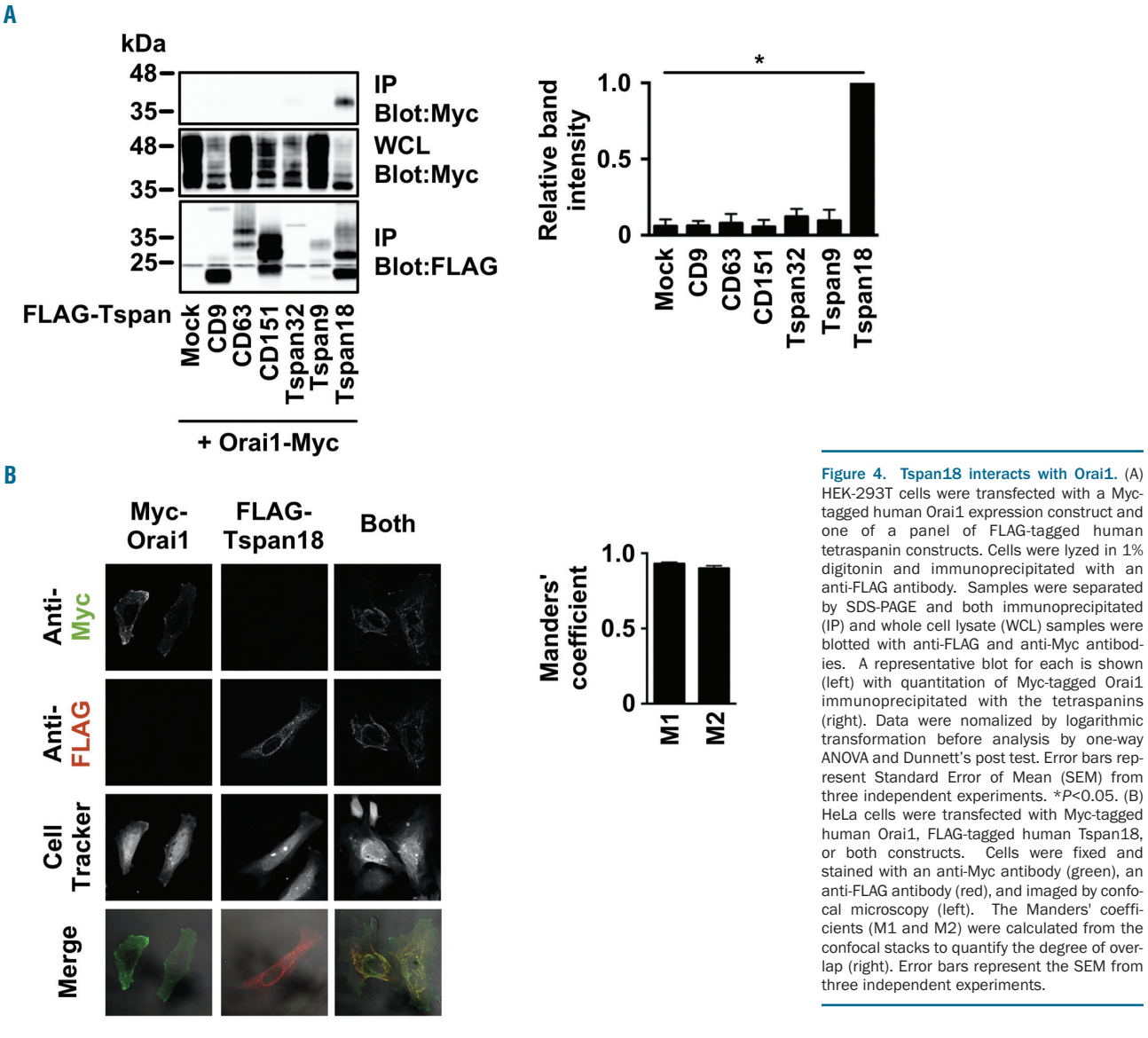

Figure 4. Tspan18 interacts with Orai1. (A) HEK-293T cells were transfected with a Myc-tagged human Orai1 expression construct and one of a panel of FLAG-tagged human tetraspanin constructs. Cells were lyzed in 1% digitonin and immunoprecipitated with an anti-FLAG antibody. Samples were separated by SDS-PAGE and both immunoprecipitated (IP) and whole cell lysate (WCL) samples were blotted with anti-FLAG and anti-Myc antibodies. A representative blot for each is shown (left) with quantitation of Myc-tagged Orai1 immunoprecipitated with the tetraspanins (right). Data were nomalized by logarithmic transformation before analysis by one-way ANOVA and Dunnett's post test. Error bars represent Standard Error of Mean (SEM) from three independent experiments. *$P<0.05$. (B) HeLa cells were transfected with Myc-tagged human Orai1, FLAG-tagged human Tspan18, or both constructs. Cells were fixed and stained with an anti-Myc antibody (green), an anti-FLAG antibody (red), and imaged by confocal microscopy (left). The Manders' coefficients (M1 and M2) were calculated from the confocal stacks to quantify the degree of overlap (right). Error bars represent the SEM from three independent experiments.

(Figure 6D and E). These data suggest that the impaired hemostasis phenotype is due to a defect in a non-hematopoietic vascular cell type such as the endothelial cell. This did not appear to be due to any observable structural defects in the vasculature, because immunohistochemistry analyses of blood vessels in organs such as kidney and pancreas were similar for wild-type and Tspan18-knockout mice (Figure 6F), as were immunofluorescence analyses of blood vessels in the ear (Figure 6G).

Tspan18 and Orai1 are required for endothelial release of von Willebrand factor in response to inflammatory mediators

Endothelial cell stimulation by inflammatory agonists induces vWF release from Weibel-Palade bodies *via* a process that involves Ca^{2+} signaling.[14] To investigate whether Tspan18 could be required for vWF release, HUVEC were subjected to Tspan18 knockdown and stimulated in culture medium with thrombin or hista-

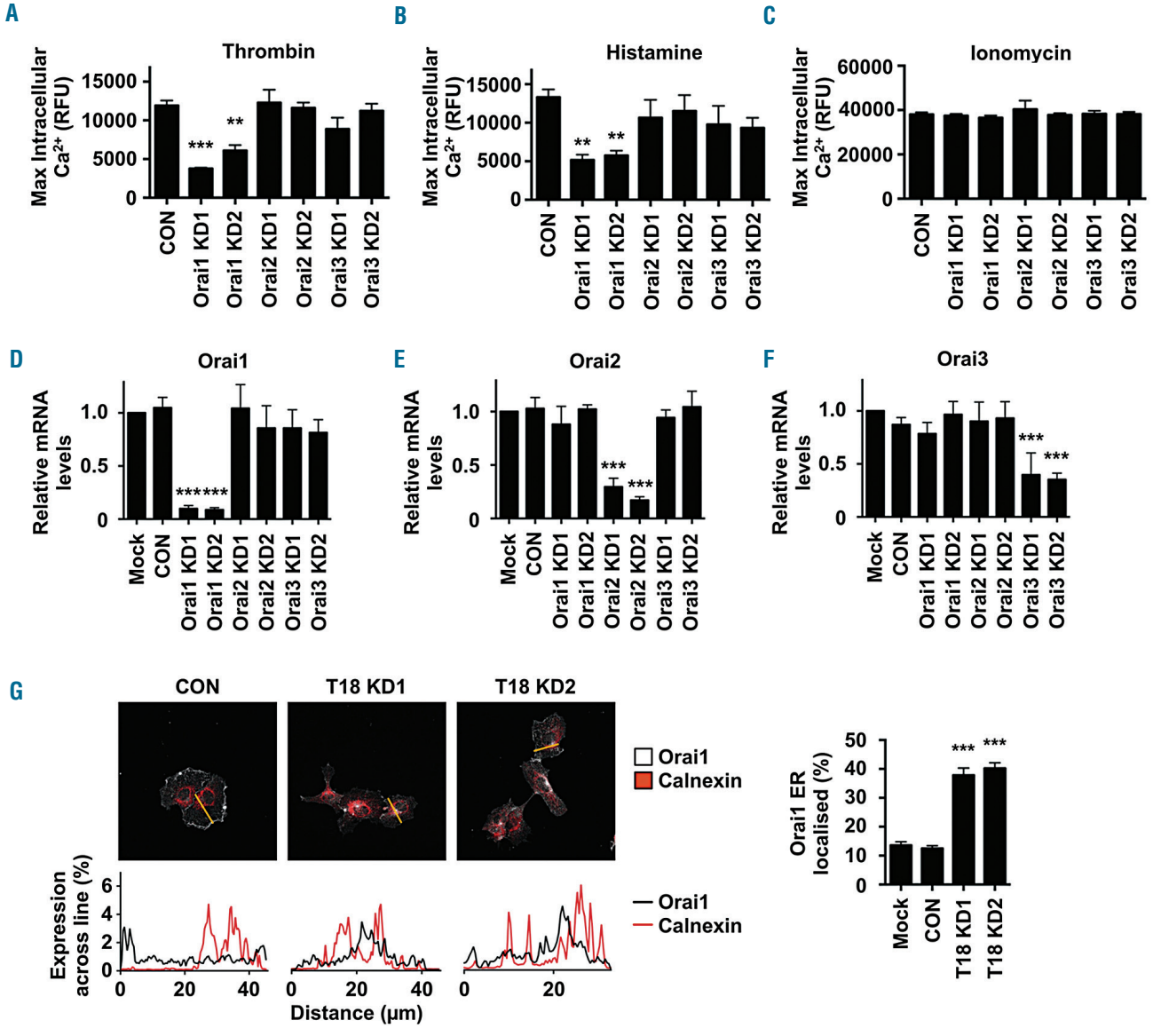

Figure 5. Orai1-knockdown endothelial cells have impaired Ca^{2+} mobilization and Orai1 surface expression requires Tspan18. (A-F) Human umbilical vein endothelial cells (HUVEC) were transfected with a negative control siRNA (CON) or with one of two independent siRNA targeting Orai1, Orai2 or Orai3 (Orai1-3 KD). After 48 hours (h), Ca^{2+} measurements were taken as described in Figure 2A-C, following addition of 1 U/mL thrombin (A), 20 μM histamine (B), or 10 μM ionomycin (C), and quantitation of maximum intracellular Ca^{2+} concentrations is shown. Error bars represent Standard Error of the Mean (SEM) from three independent experiments. $^{**}P<0.01$; $^{***}P<0.001$. (D-F) siRNA-transfected HUVEC from (A-C) were subjected to quantitative real-time polymerase chain reaction (qPCR) for Orai1 (D), Orai2 (E) or Orai3 (F), as described for Figure 2D. Error bars represent SEM from three independent experiments. $^{***}P<0.001$. (G) HUVEC lentivirally-transduced to express Myc-tagged Orai1 were treated with control or Tspan18 siRNA. Cells were stained with anti-Myc (white) or anti-calnexin endoplasmic reticulum marker (red) antibodies, and representative confocal microscopy images are shown (top). In the line graphs below the images (bottom), the percentage expression of Orai1 (black) and calnexin (red) across the yellow line in the top panel was determined using ImageJ. The percentage of Orai1 that localized to a calnexin endoplasmic reticulum mask was then quantified (right). Data were generated from 15 cells per condition from three independent experiments (five cells per condition per experiment). Error bars represent SEM. $^{***}P<0.001$. RFU: relative fluorescence unit.

mine. Soluble vWF release, as detected by ELISA, was reduced by approximately 90% compared to control cells (Figure 7A). This was corroborated by immunofluorescent staining of vWF that showed minimal release of Weibel-Palade bodies after Tspan18 knockdown (Figure 7B). Similar to Tspan18, Orai1 knockdown reduced Weibel-Palade body release after thrombin stimulation, but knockdown of Orai2 or Orai3 had no effect (Figure 7C). Furthermore, Tspan18 knockdown reduced platelet adhesion to a thrombin-activated HUVEC monolayer by 85-90% (Figure 7D). These data support a role for Tspan18 and Orai1 in vWF release and platelet capture following endothelial cell activation by inflammatory mediators.

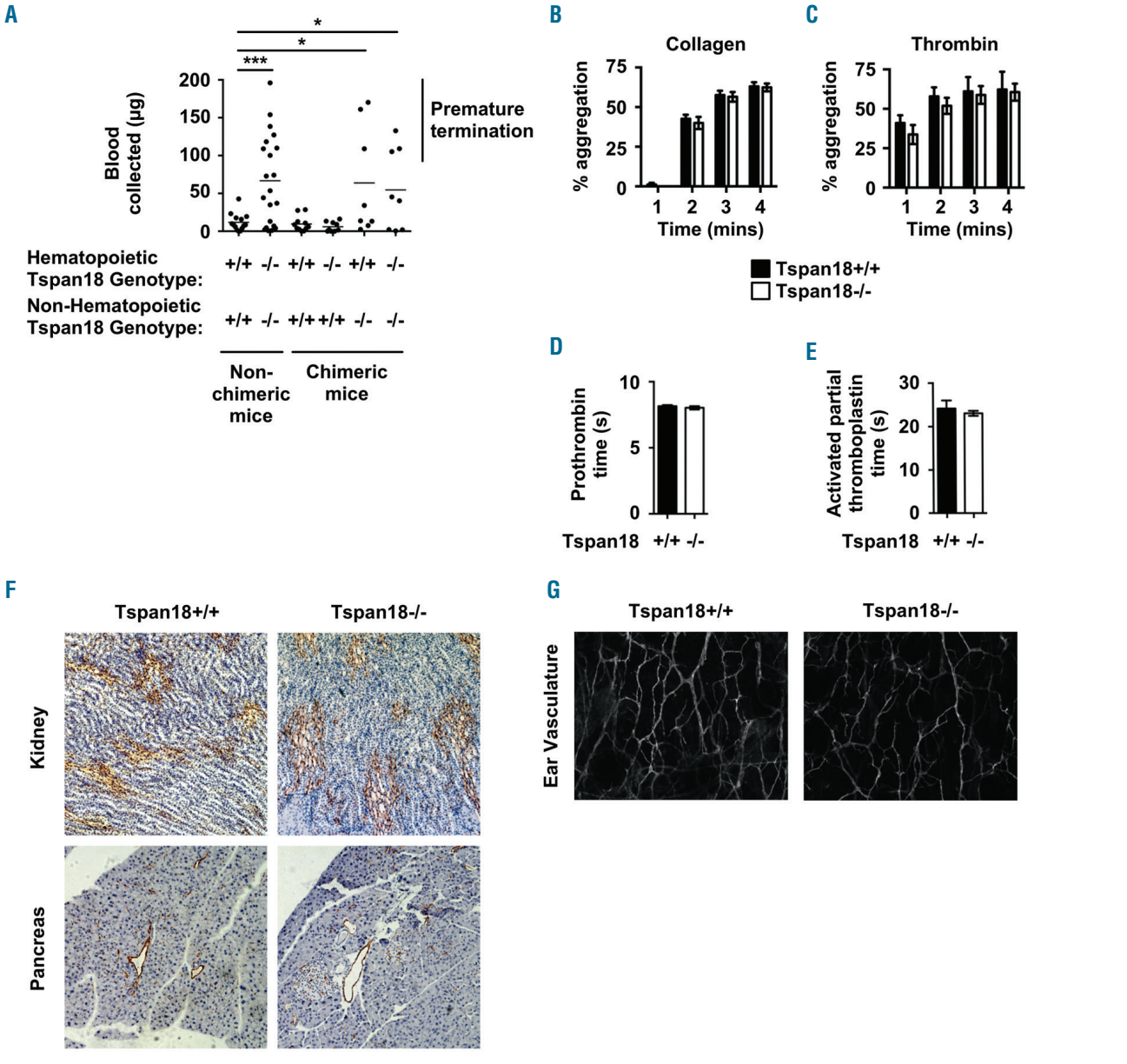

Figure 6. Tspan18-knockout mice have a hemostasis defect due to the absence of Tspan18 expression by non-hematopoietic cells. (A) Tail bleeding assays were performed by amputating 3 mm tail tips of anesthetized mice and the weight of blood lost was measured. The mice were Tspan18$^{+/+}$, Tspan18$^{-/-}$, or lethally irradiated Tspan18$^{-/-}$ or Tspan18$^{+/+}$ mice reconstituted with fetal liver cells from Tspan18$^{+/+}$ or Tspan18$^{-/-}$ embryos. Each symbol represents one animal. All data were analyzed by Fisher's exact test. *P<0.05; ***P<0.001. Note that bleeding was stopped by cauterizing the tails of some mice, because of regulations limiting the amount of blood loss on our Home Office License. (B and C) Washed platelets from Tspan18$^{+/+}$ or Tspan18$^{-/-}$ mice were activated with 3 µg/mL collagen (B) or 0.3 U/mL thrombin (C), and aggregation was measured by light transmission with stirring. Quantitated percentage aggregation each minute is shown. Error bars represent the Standard Error of Mean (SEM) from at least three pairs of litter-matched mice. (D and E) Plasma samples from Tspan18$^{+/+}$ and Tspan18$^{-/-}$ mice were subjected to a prothrombin time test with human placental thromboplastin (D) and an activated partial thromboplastin time test with purified soy phosphatides with ellagic acid (E). Error bars represent SEM from four pairs of litter-matched mice. (F) Immunohistochemistry was used to show a grossly normal vasculature in Tspan18$^{+/+}$ and Tspan18$^{-/-}$ mice formalin-fixed paraffin-embedded 5 µm sections from kidney and pancreas, using the MECA32 anti-mouse panendothelial cell antibody. Images are representative of three pairs of litter-matched mice. (G) Confocal microscopy was used to show a grossly normal vasculature in Tspan18$^{+/+}$ and Tspan18$^{-/-}$ mice ears, by staining anterior ear tissue with biotinylated isolectin GS-IB4 glycoprotein followed by Alexa647-conjugated streptavidin. Images are representative of three pairs of litter-matched mice. ImageJ quantitation of 3 fields of view (500 x 500 pixels) per mouse showed a mean total vessel length of 11131±1271 pixels for Tspan18$^{+/+}$ and 11684±283 pixels for Tspan18$^{-/-}$ (n=3; error represents SEM). mins: minutes.

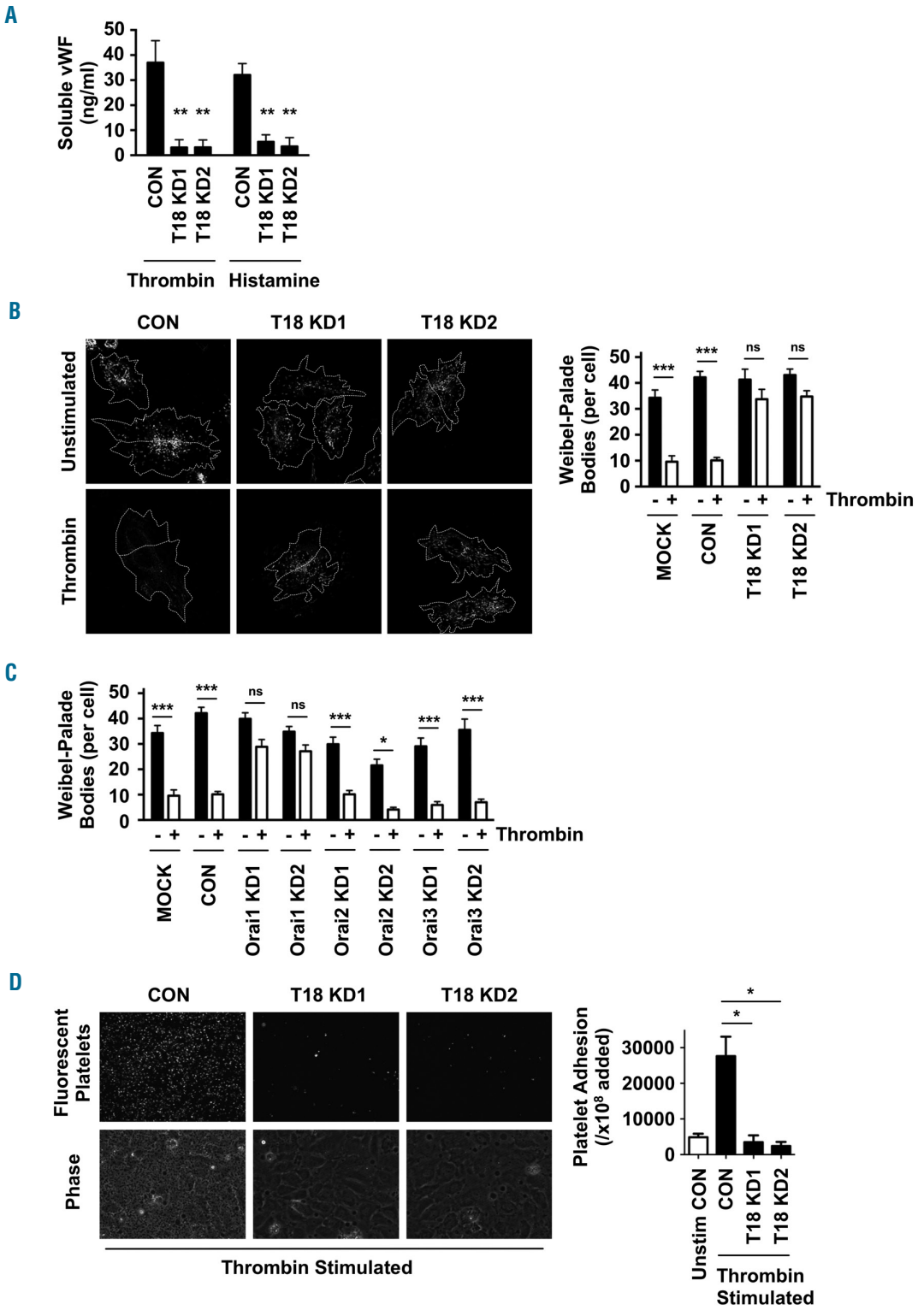

Figure 7. Tspan18-knockdown endothelial cells have impaired histamine- and thrombin-induced release of von Willebrand Factor (vWF). (A) Human umbilical vein endothelial cells (HUVEC) were transfected with a negative control siRNA (CON) or with one of two independent siRNA targeting Tspan18 (T18 KD). After 48 hours, HUVEC were stimulated with 1 U/mL thrombin or 20 μM histamine for 5 minutes (min). Cultured media was removed and assayed for vWF by ELISA. Pre-stimulation levels of vWF were subtracted from these data. Error bars represent the Standard Error of Mean (SEM) from three experiments. $^{**}P<0.01$. (B) HUVEC transfected as described in (A) were stimulated with 1 U/mL thrombin for 5 min, and the cells were fixed and stained with an anti-vWF antibody followed by Alexa488-conjugated secondary antibody. Representative confocal microscopy images are shown (left). Z-stack images were de-noised, background-subtracted and analyzed for the number of vWF cellular bodies, using ImageJ. Counts were made on 5-10 cells per experiment for four independent experiments (right panel). Error bars represent Standard Error of Mean (SEM). $^{***}P<0.001$; ns: not significant. (C) The experiment and quantitation was conducted as for (B), except that HUVEC were mock-transfected with no siRNA (Mock), transfected with negative control siRNA (CON), or siRNA to Orai1, Orai2 or Orai3 (KD). (D) HUVEC were siRNA-transfected and stimulated with 1 U/mL thrombin for 5 min as described in (A). Human washed platelets were fluorescently labeled and incubated with the HUVEC monolayers. Non-adherent platelets were removed by washing and images were collected. Representative fluorescent images of adhered platelets (top) and phase contrast images of the HUVEC monolayers and adhered platelets (bottom) are shown, with quantitation of platelet adhesion from three independent experiments (right). Error bars represent SEM. $^{*}P<0.05$.

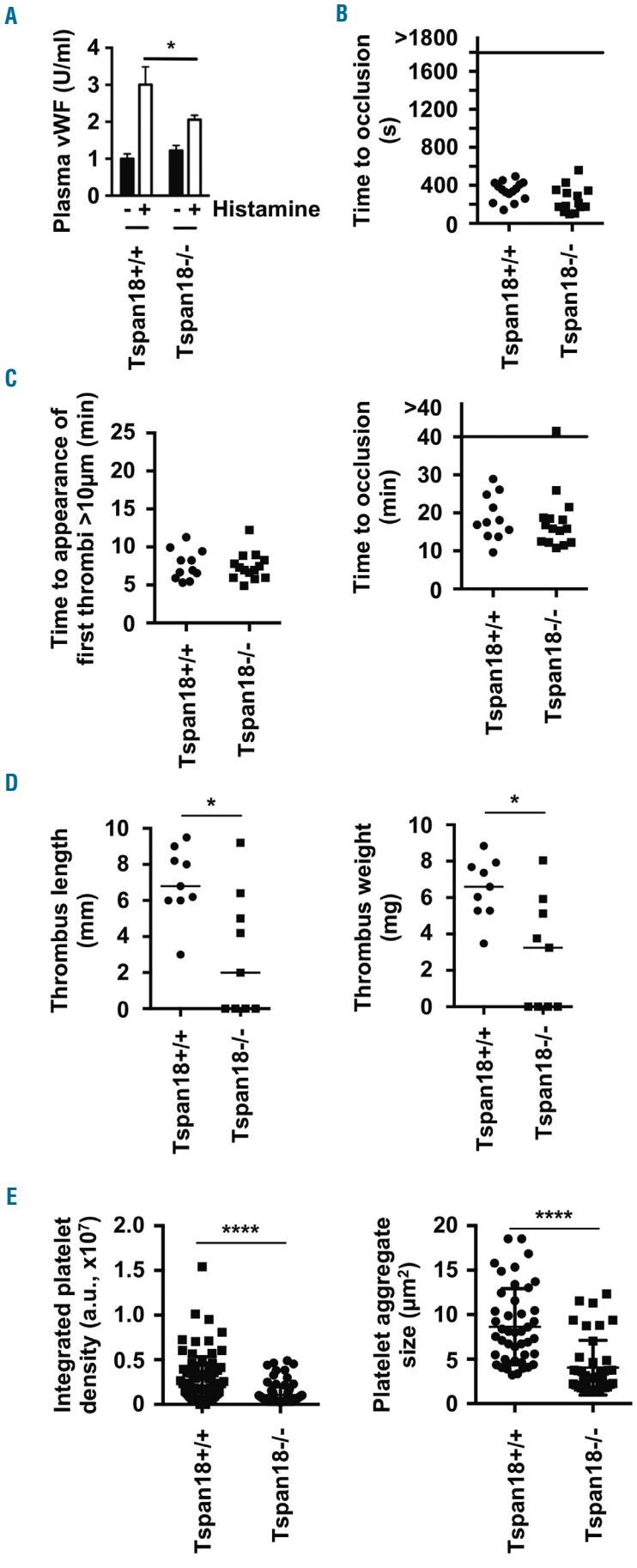

Figure 8. Tspan18-knockout mice have impaired histamine-induced von Willebrand Factor (vWF) release and impaired thrombo-inflammatory responses. (A) Tspan18$^{+/+}$ and Tspan18$^{-/-}$ mice were intraperitoneally-injected with histamine and plasma vWF levels were measured 30 minutes (min) later by ELISA. Error bars represent Standard Error of Mean (SEM) from eight Tspan18$^{+/+}$ and seven Tspan18$^{-/-}$ mice. *P<0.05. (B) Tspan18$^{+/+}$and Tspan18$^{-/-}$ mice were anesthetized, and the abdominal aorta exposed and mechanically injured through a single firm compression with forceps. Blood flow was subsequently monitored with a Doppler flowmeter to calculate the time until complete occlusion of the vessel. Each symbol represents one animal. (C) Tspan18$^{+/+}$ and Tspan18$^{-/-}$ mice were anesthetized and the mesentery was exteriorized through an abdominal incision. Platelets were fluorescently labeled with Dylight 488-conjugated anti-GPIX derivative. Small mesenteric arterioles were exposed to $FeCl_3$-induced chemical injury *via* topical application. Time to appearance of the first thrombi was recorded (left), and the time until complete occlusion of the vessel was measured using fluorescence intravital microscopy (right). Each symbol represents one animal. (D) Tspan18$^{+/+}$ and Tspan18$^{-/-}$ mice were anesthetized and surgery performed to stenose the inferior vena cava. After 48 hours (h), thrombus length (left) and weight (right) were measured. Each symbol represents one animal and horizontal bars represent the median. *P<0.05. All data in (A-D) were analyzed by one-way ANOVA with Dunnett's multiple comparisons test. (E) Myocardial ischemia-reperfusion injury was induced in the left ventricle of the beating heart of anesthetized mice by occluding the left anterior descending artery for 45 min with a suture. Reperfusion was instigated for 2 h by removal of the ligature, after which the organ was harvested. Frozen sections were analyzed for the presence of platelets in the microcirculation by immunofluorescence microscopy. Three litter-matched pairs of Tspan18$^{+/+}$ and Tspan18$^{-/-}$ mice were used, with three sections per mouse and five images analyzed per section. Each symbol represents one image. For each image, the integrated density value was calculated as a representation of the total number of platelets (left), and the average aggregate size was also calculated (right). Error bars represent the SEM and data were analyzed by Mann-Whitney test. ****P<0.0001.

Tspan18-knockout mice have impaired histamine-induced release of endothelial von Willebrand factor and impaired thrombo-inflammatory responses

To determine whether Tspan18 has a role in vWF release *in vivo*, Tspan18-knockout mice were intra-peritoneally injected with histamine, and plasma vWF levels were analyzed by ELISA. Induced plasma vWF release was reduced by approximately 50% in the absence of Tspan18 (Figure 8A). Basal plasma vWF was normal in Tspan18-knockout mice (Figure 8A), indicating a requirement for Tspan18 in regulated, but not basal, vWF release.

To investigate the role of Tspan18 in thrombosis, two arterial thrombosis models and two thrombo-inflammatory models were used. In a platelet-driven aorta injury arterial thrombosis model,[38] no difference in time to complete occlusion of the vessel between Tspan18-knockout and wild-type littermate control mice was observed (Figure 8B). Similarly, there was no thrombosis defect in mesenteric arterioles following application of $FeCl_3$ (Figure 8C), which is also a platelet-driven model,[38] but shows reduced platelet deposition and thrombus formation in the complete absence of vWF.[53,54] In a deep vein thrombosis thrombo-inflammatory model that is dependent on endothelial vWF,[13] thrombus length and weight were reduced by approximately 60% in the Tspan18-knockout mice, compared to wild-type littermate controls (Figure 8D). Moreover, 4 of 9 Tspan18-knockout mice failed to develop a thrombus compared to 100% thrombus formation in wild-type mice (Figure 8D). Macroscopically, thrombi from Tspan18-knockout mice had similar red and white parts to those from wild-type mice (*data not shown*). Finally, in a vWF-dependent myocardial ischemia-reperfusion thrombo-inflammatory model,[55,56] platelet deposition and aggregate size in the microcirculation were reduced by approximately 50% (Figure 8E). The reduction in severity in the two thrombo-inflammatory models is consistent with the requirement of Tspan18 for endothelial vWF release in response to inflammatory mediators.

Discussion

We have discovered that Tspan18 is expressed by endothelial cells and interacts with the SOCE channel Orai1. Tspan18-knockdown endothelial cells had reduced Orai1 expression at the cell surface and impaired Ca^{2+} signaling. This is consistent with the established role of tetraspanins in interacting with specific partner proteins in the ER, and promoting their trafficking to the cell surface,[1,50,51] albeit *via* mechanisms that are yet to be defined. Tspan18 is not particularly related to any of the other 32 mammalian tetraspanins,[22] suggesting that it may be unique amongst tetraspanins in regulating Orai1. Indeed, none of the five tetraspanins that were selected as controls interacted with Orai1, or induced Ca^{2+}-responsive NFAT activation, when over-expressed.

At the cell surface, tetraspanins can regulate the lateral diffusion and clustering of their partner proteins.[2,3] A question that arises from the present study is whether Tspan18 regulates Orai1 clustering at the endothelial cell surface. Interestingly, a unimolecular coupling model of Orai1 activation was recently proposed, whereby one molecule of a STIM1 dimer is sufficient to induce opening of the Orai1 hexamer channel.[10] This would enable the other STIM1 molecule in the dimer to cross-link with a second Orai1 hexamer and form a lattice of clustered Orai1 channels. The degree of cluster formation could dictate the kinetics of channel activation and could concentrate Ca^{2+} influx to particular regions of the plasma membrane.[10] This could affect the extent to which downstream effectors are activated. Tetraspanins have been reported to exist as nanodomains of approximately ten tetraspanins of a single type,[57] therefore Tspan18 may cluster Orai1 into pre-formed nanodomains, so modulating Orai1 lattice formation by STIM1. This may provide a means by which endothelial cells fine-tune SOCE and downstream functional responses. It remains to be determined whether Tspan18 also regulates Orai2 and Orai3, but we found no role for these Orai family members in inflammatory mediator-induced HUVEC Ca^{2+} mobilization, consistent with other studies.[48,49]

The inflammatory mediators thrombin and histamine activate G protein-coupled receptors to induce downstream Ca^{2+} mobilization and the release of vWF from Weibel-Palade bodies.[14] Consistent with impaired Ca^{2+} signaling, Tspan18-knockout endothelial cells had impaired inflammatory mediator-induced vWF release *in vitro* and *in vivo*. In contrast, basal release of vWF appeared to be normal, because basal plasma vWF levels were unaffected in Tspan18-knockout mice. We hypothesize that impaired vWF release, in response to inflammatory mediators, explains the *in vivo* phenotypes observed in Tspan18-knockout mice. The protection from deep vein thrombosis is consistent with the central role of vWF in this disease.[13] Furthermore, the reduced platelet deposition in the microcirculation during myocardial ischemia-reperfusion injury is consistent with the role of vWF in this process.[55,56] The hemostasis defect still needs to be explained, because although a tail bleeding phenotype has been demonstrated in endothelial-specific vWF-knockout mice, these animals also had low plasma vWF,[58,59] unlike Tspan18 knockouts. The tail bleeding assay measures blood loss following excision of the tip of the tail, which contains the two lateral veins, the dorsal vein, and the ventral artery. We speculate that endothelial cells in the veins and artery, adjacent to the site of excision, are activated and release vWF *via* Ca^{2+}-dependent signaling. The vWF may trap platelets, facilitating their aggregation and preventing excessive blood loss from the site of tail injury. Therefore, our data suggest that acute release of vWF adjacent to a site of injury might be important for hemostasis, at least for some types of injury. Finally, the lack of a phenotype in the two arterial thrombosis models is consistent with the importance of platelets in these models,[38] and we found no defect in aggregation *in vitro* for Tspan18-knockout platelets.

In summary, we have identified Tspan18 as a novel regulator of endothelial Orai1 and SOCE. Our *in vivo* data show that Tspan18 regulates inflammation-induced vWF release but not basal release, and promotes hemostasis and thrombo-inflammatory processes but not arterial thrombosis.

Acknowledgments

We are grateful to Carl Blobel, Chris Bunce, Dean Kavanagh, Neil Morgan and Steve Publicover for their helpful comments on this project. We thank the Birmingham Biomedical Sciences Unit for maintaining mice, and the Birmingham Advanced Light Microscope Facility for imaging expertise.

Funding

This work was funded by a British Heart Foundation Project Grant (PG/13/92/30587) which supported PJN, Biotechnology and Biological Sciences Research Council PhD Studentships which supported RLG and EJH, British Heart Foundation PhD Studentships which supported DC, JSR and CZK (FS/05/048, FS/12/79/29871 and FS/18/9/33388), a British Heart Foundation Senior Fellowship (FS/08/062/25797) to MGT which also supported JY, a Biotechnology and Biological Sciences Research Council Project Grant (BB/P00783X/1) which supported NH and a Medical Research Council New Investigator Award (RRAK10717) which supported MGT. SPW is a British Heart Foundation Chair (CH03/003).

References

1. Matthews AL, Szyroka J, Collier R, Noy PJ, Tomlinson MG. Scissor sisters: regulation of ADAM10 by the TspanC8 tetraspanins. Biochem Soc Trans. 2017;45(3):719-730.
2. Termini CM, Gillette JM. Tetraspanins Function as Regulators of Cellular Signaling. Front Cell Dev Biol. 2017;5:34.
3. van Deventer SJ, Dunlock VE, van Spriel AB. Molecular interactions shaping the tetraspanin web. Biochem Soc Trans. 2017;45(3):741-750.
4. Zimmerman B, Kelly B, McMillan BJ, et al. Crystal Structure of a Full-Length Human Tetraspanin Reveals a Cholesterol-Binding Pocket. Cell. 2016;167(4):1041-1051.
5. Fairchild CL, Conway JP, Schiffmacher AT, Taneyhill LA, Gammill LS. FoxD3 regulates cranial neural crest EMT via downregulation of tetraspanin18 independent of its functions during neural crest formation. Mech Dev. 2014;132:1-12.
6. Fairchild CL, Gammill LS. Tetraspanin18 is a FoxD3-responsive antagonist of cranial neural crest epithelial-to-mesenchymal transition that maintains cadherin-6B protein. J Cell Sci. 2013;126(Pt 6):1464-1476.
7. Putney JW, Steinckwich-Besancon N, Numaga-Tomita T, et al. The functions of store-operated calcium channels. Biochim Biophys Acta. 2017;1864(6):900-906.
8. Trebak M, Putney JW Jr. ORAI Calcium Channels. Physiology (Bethesda). 2017; 32(4):332-342.
9. Yeung PS, Yamashita M, Prakriya M. Pore opening mechanism of CRAC channels. Cell Calcium. 2017;63:14-19.
10. Zhou Y, Cai X, Nwokonko RM, Loktionova NA, Wang Y, Gill DL. The STIM-Orai coupling interface and gating of the Orai1 channel. Cell Calcium. 2017;63:8-13.
11. Gragnano F, Sperlongano S, Golia E, et al. The Role of von Willebrand Factor in Vascular Inflammation: From Pathogenesis to Targeted Therapy. Mediators Inflamm. 2017;2017:5620314.
12. Kawecki C, Lenting PJ, Denis CV. von Willebrand factor and inflammation. J Thromb Haemost. 2017;15(7):1285-1294.
13. Brill A, Fuchs TA, Chauhan AK, et al. von Willebrand factor-mediated platelet adhesion is critical for deep vein thrombosis in mouse models. Blood. 2011;117(4):1400-1407.
14. McCormack JJ, Lopes da Silva M, Ferraro F, Patella F, Cutler DF. Weibel-Palade bodies at a glance. J Cell Sci. 2017;130(21):3611-3617.
15. Brill A, Fuchs TA, Savchenko AS, et al. Neutrophil extracellular traps promote deep vein thrombosis in mice. J Thromb Haemost. 2012;10(1):136-144.
16. Ponomaryov T, Payne H, Fabritz L, Wagner DD, Brill A. Mast Cells Granular Contents Are Crucial for Deep Vein Thrombosis in Mice. Circ Res. 2017;121(8):941-950.
17. von Bruhl ML, Stark K, Steinhart A, et al. Monocytes, neutrophils, and platelets cooperate to initiate and propagate venous thrombosis in mice in vivo. J Exp Med. 2012;209(4):819-835.
18. Tang T, Li L, Tang J, et al. A mouse knockout library for secreted and transmembrane proteins. Nat Biotechnol. 2010;28(7):749-755.
19. Hughes CE, Navarro-Nunez L, Finney BA, Mourao-Sa D, Pollitt AY, Watson SP. CLEC-2 is not required for platelet aggregation at arteriolar shear. J Thromb Haemost. 2010;8(10):2328-2332.
20. Shapiro VS, Truitt KE, Imboden JB, Weiss A. CD28 mediates transcriptional upregulation of the interleukin-2 (IL-2) promoter through a composite element containing the CD28RE and NF-IL-2B AP-1 sites. Mol Cell Biol. 1997;17(7):4051-4058.
21. Tomlinson MG, Calaminus SD, Berlanga O, et al. Collagen promotes sustained glycoprotein VI signaling in platelets and cell lines. J Thromb Haemost. 2007;5(11):2274-2283.
22. Haining EJ, Yang J, Bailey RL, et al. The TspanC8 subgroup of tetraspanins interacts with A disintegrin and metalloprotease 10 (ADAM10) and regulates its maturation and cell surface expression. J Biol Chem. 2012;287(47):39753-39765.
23. Protty MB, Watkins NA, Colombo D, et al. Identification of Tspan9 as a novel platelet tetraspanin and the collagen receptor GPVI as a component of tetraspanin microdomains. Biochem J. 2009;417(1):391-400.
24. Gwack Y, Srikanth S, Feske S, et al. Biochemical and functional characterization of Orai proteins. J Biol Chem. 2007;282(22):16232-16243.
25. O'Keefe SJ, Tamura J, Kincaid RL, Tocci MJ, O'Neill EA. FK-506- and CsA-sensitive activation of the interleukin-2 promoter by calcineurin. Nature. 1992;357(6380):692-694.
26. Sugawara H, Kurosaki M, Takata M, Kurosaki T. Genetic evidence for involvement of type 1, type 2 and type 3 inositol 1,4,5-trisphosphate receptors in signal transduction through the B-cell antigen receptor. Embo J. 1997;16(11):3078-3088.
27. Ehrhardt C, Schmolke M, Matzke A, et al. Polyethylenimine, a cost-effective transfection reagent. Signal Transduction. 2006;6:179–184.
28. Noy PJ, Yang J, Reyat JS, et al. TspanC8 Tetraspanins and A Disintegrin and Metalloprotease 10 (ADAM10) Interact via Their Extracellular Regions: EVIDENCE FOR DISTINCT BINDING MECHANISMS FOR DIFFERENT TspanC8 PROTEINS. J Biol Chem. 2016;291(7):3145-3157.
29. Wilson E, Leszczynska K, Poulter NS, et al. RhoJ interacts with the GIT-PIX complex and regulates focal adhesion disassembly. J Cell Sci. 2014;127(Pt 14):3039-3051.
30. Pfaffl MW. A new mathematical model for relative quantification in real-time RT-PCR. Nucleic Acids Res. 2001;29(9):e45.
31. Reyat JS, Tomlinson MG, Noy PJ. Utilizing Lentiviral Gene Transfer in Primary Endothelial Cells to Assess Lymphocyte-Endothelial Interactions. Methods Mol Biol. 2017;1591:155-168.
32. Manders EMM, Verbeek FJ, Aten JA. Measurement of Colocalization of Objects in Dual-Color Confocal Images. J Microsc-Oxford. 1993;169:375-382.
33. Gardenier JC, Hespe GE, Kataru RP, et al. Diphtheria toxin-mediated ablation of lymphatic endothelial cells results in progressive lymphedema. JCI Insight. 2016;1(15): e84095.
34. Simms V, Bicknell R, Heath VL. Development of an ImageJ-based method for analysing the developing zebrafish vasculature. Vascular Cell. 2017;9(1):2.
35. Parsonage G, Machado LR, Hui JW, et al. CXCR6 and CCR5 localize T lymphocyte subsets in nasopharyngeal carcinoma. Am J Pathol. 2012;180(3):1215-1222.
36. Pollitt AY, Poulter NS, Gitz E, et al. Syk and Src family kinases regulate C-type lectin receptor 2 (CLEC-2)-mediated clustering of podoplanin and platelet adhesion to lymphatic endothelial cells. J Biol Chem. 2014;289(52):35695-35710.
37. Senis YA, Tomlinson MG, Ellison S, et al. The tyrosine phosphatase CD148 is an essential positive regulator of platelet activation and thrombosis. Blood. 2009;113:4942-4954.
38. Braun A, Varga-Szabo D, Kleinschnitz C, et al. Orai1 (CRACM1) is the platelet SOC channel and essential for pathological thrombus formation. Blood. 2009; 113(9):2056-2063.
39. Xu Z, Alloush J, Beck E, Weisleder N. A murine model of myocardial ischemia-reperfusion injury through ligation of the left anterior descending artery. J Vis Exp. 2014(86).
40. Du Y, Kitzmiller JA, Sridharan A, et al. Lung Gene Expression Analysis (LGEA): an integrative web portal for comprehensive gene expression data analysis in lung development. Thorax. 2017;72(5):481-484.
41. Zhang Y, Chen K, Sloan SA, et al. An RNA-sequencing transcriptome and splicing database of glia, neurons, and vascular cells of the cerebral cortex. The Journal of neuroscience : the official journal of the Society for Neuroscience. 2014;34(36):11929-11947.
42. Uhlen M, Fagerberg L, Hallstrom BM, et al. Proteomics. Tissue-based map of the human proteome. Science. 2015;347(6220):1260419.
43. Fuller GL, Williams JA, Tomlinson MG, et al. The C-type lectin receptors CLEC-2 and Dectin-1, but not DC-SIGN, signal via a novel YXXL-dependent signaling cascade. J Biol Chem. 2007;282(17):12397-12409.
44. Prakriya M, Feske S, Gwack Y, Srikanth S,

Rao A, Hogan PG. Orai1 is an essential pore subunit of the CRAC channel. Nature. 2006;443(7108):230-233.
45. Vig M, Beck A, Billingsley JM, et al. CRACM1 multimers form the ion-selective pore of the CRAC channel. Curr Biol. 2006;16(20):2073-2079.
46. Yeromin AV, Zhang SL, Jiang W, Yu Y, Safrina O, Cahalan MD. Molecular identification of the CRAC channel by altered ion selectivity in a mutant of Orai. Nature. 2006;443(7108):226-229.
47. Dornier E, Coumailleau F, Ottavi JF, et al. TspanC8 tetraspanins regulate ADAM10/Kuzbanian trafficking and promote Notch activation in flies and mammals. J Cell Biol. 2012;199(3):481-496.
48. Li J, Cubbon RM, Wilson LA, et al. Orai1 and CRAC channel dependence of VEGF-activated Ca2+ entry and endothelial tube formation. Circ Res. 2011;108(10):1190-1198.
49. Zhou MH, Zheng H, Si H, et al. Stromal interaction molecule 1 (STIM1) and Orai1 mediate histamine-evoked calcium entry and nuclear factor of activated T-cells (NFAT) signaling in human umbilical vein endothelial cells. J Biol Chem. 2014; 289(42):29446-29456.
50. Saint-Pol J, Eschenbrenner E, Dornier E, Boucheix C, Charrin S, Rubinstein E. Regulation of the trafficking and the function of the metalloprotease ADAM10 by tetraspanins. Biochem Soc Trans. 2017; 45(4):937-944.
51. Vences-Catalan F, Duault C, Kuo CC, Rajapaksa R, Levy R, Levy S. CD81 as a tumor target. Biochem Soc Trans. 2017; 45(2):531-535.
52. Cheli Y, Jensen D, Marchese P, et al. The Modifier of hemostasis (Mh) locus on chromosome 4 controls in vivo hemostasis of Gp6-/- mice. Blood. 2008;111(3):1266-1273.
53. Denis C, Methia N, Frenette PS, et al. A mouse model of severe von Willebrand disease: defects in hemostasis and thrombosis. Proc Natl Acad Sci U S A. 1998;95(16):9524-9529.
54. Ni H, Denis CV, Subbarao S, et al. Persistence of platelet thrombus formation in arterioles of mice lacking both von Willebrand factor and fibrinogen. J Clin Invest. 2000;106(3):385-392.
55. De Meyer SF, Savchenko AS, Haas MS, et al. Protective anti-inflammatory effect of ADAMTS13 on myocardial ischemia/reperfusion injury in mice. Blood. 2012; 120(26):5217-5223.
56. Gandhi C, Motto DG, Jensen M, Lentz SR, Chauhan AK. ADAMTS13 deficiency exacerbates VWF-dependent acute myocardial ischemia/reperfusion injury in mice. Blood. 2012;120(26):5224-5230.
57. Zuidscherwoude M, Gottfert F, Dunlock VM, Figdor CG, van den Bogaart G, van Spriel AB. The tetraspanin web revisited by super-resolution microscopy. Sci Rep. 2015; 5:12201.
58. Kanaji S, Fahs SA, Shi Q, Haberichter SL, Montgomery RR. Contribution of platelet vs. endothelial VWF to platelet adhesion and hemostasis. J Thromb Haemost. 2012; 10(8):1646-1652.
59. Verhenne S, Denorme F, Libbrecht S, et al. Platelet-derived VWF is not essential for normal thrombosis and hemostasis but fosters ischemic stroke injury in mice. Blood. 2015; 126(14):1715-1722.